AD-A117 631 RUTGERS - THE STATE UNIV NEW BRUNSWICK N J DEPT OF M--ETC F/G 14/2
NONDESTRUCTIVE METHOD FOR DETERMINING FATIGUE AND STRESS-CORROS--ETC(U)
JUL 82 I R KRAMER, S WEISSMANN N00600-77-C-1134

UNCLASSIFIED DTNSRDC-82/051 NL

END
DATE FILMED
09-82
DTIC

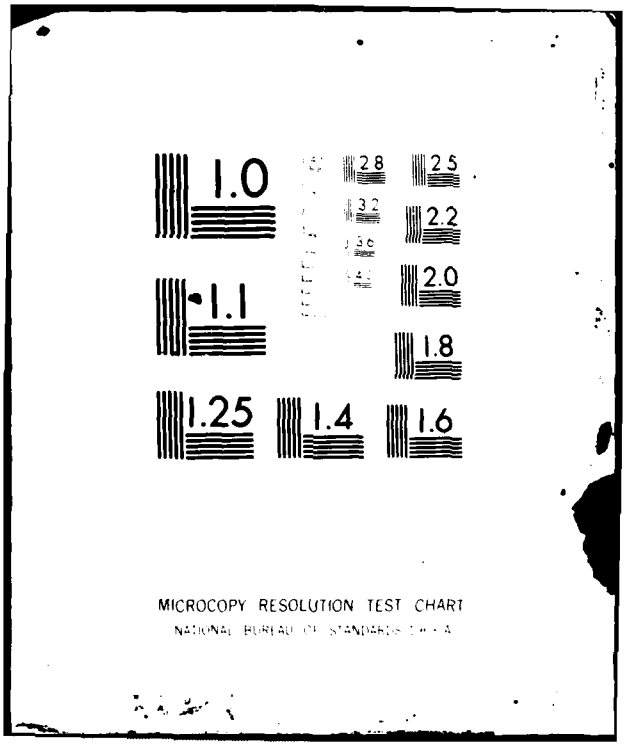
1.0
1.1
1.25
1.4
1.6
1.8
2.0
2.2
2.5
2.8
3.2
3.6
4.0
MICROCOPY RESOLUTION TEST CHART
NATIONAL BUREAU OF STANDARDS 1963-A

DAVID W. TAYLOR NAVAL SHIP RESEARCH AND DEVELOPMENT CENTER

Bethesda, Maryland 20084

NONDESTRUCTIVE METHOD FOR DETERMINING FATIGUE AND STRESS-CORROSION DAMAGE

by

I.R. Kramer
and
S. Weissmann
Professor, Department of Mechanics and Material Science
College of Engineering
Piscataway, New Jersey 08854

SHIP MATERIALS ENGINEERING DEPARTMENT
RESEARCH AND DEVELOPMENT REPORT

July 1982

DTNSRDC-82/051

MAJOR DTNSRDC ORGANIZATIONAL COMPONENTS

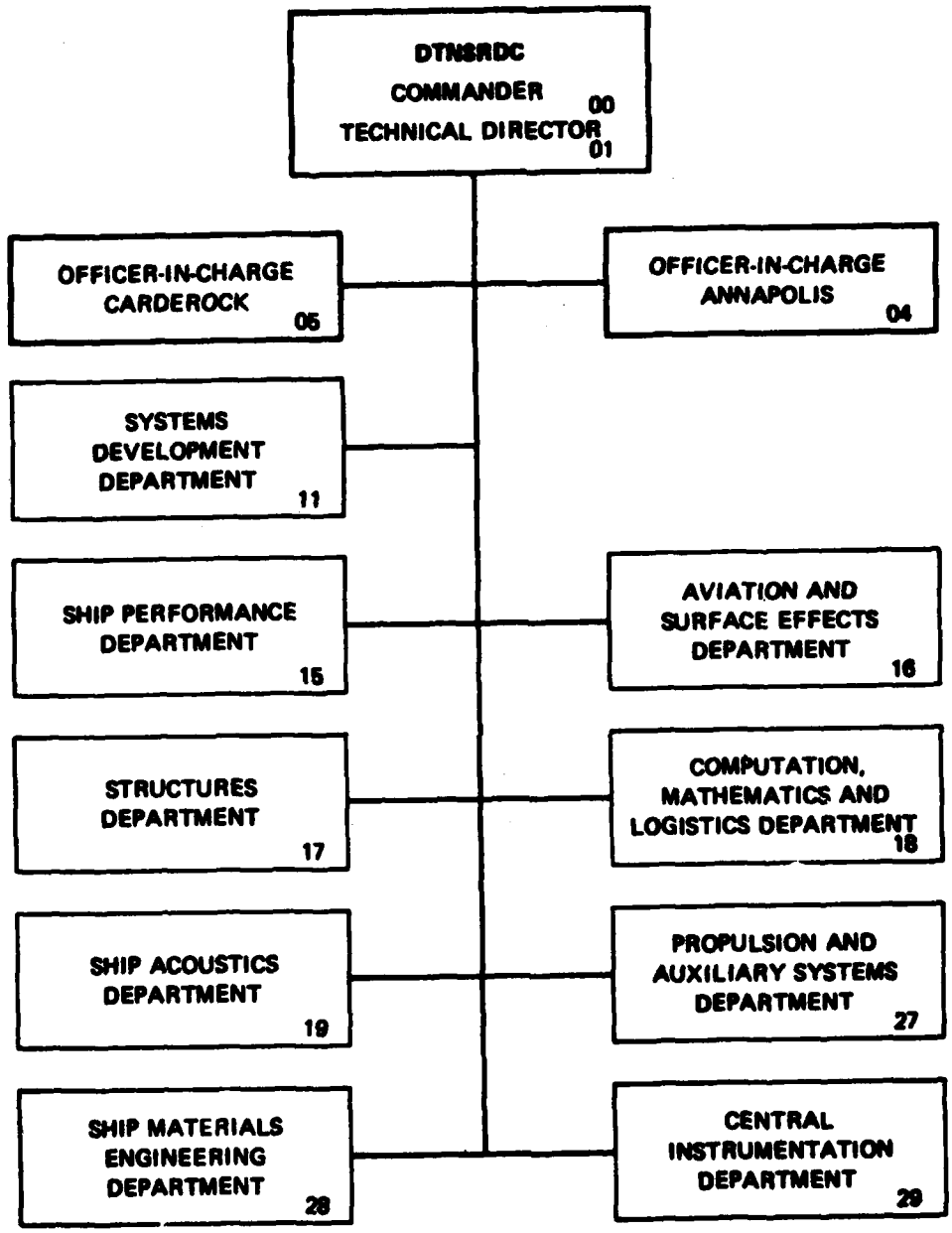

UNCLASSIFIED

SECURITY CLASSIFICATION OF THIS PAGE (When Data Entered)

REPORT DOCUMENTATION PAGE		READ INSTRUCTIONS BEFORE COMPLETING FORM
1. REPORT NUMBER DTNSRDC-82/051	2. GOVT ACCESSION NO. AD-A117631	3. RECIPIENT'S CATALOG NUMBER
4. TITLE (and Subtitle) NONDESTRUCTIVE METHOD FOR DETERMINING FATIGUE AND STRESS-CORROSION DAMAGE		5. TYPE OF REPORT & PERIOD COVERED Final 6. PERFORMING ORG. REPORT NUMBER
7. AUTHOR(s) I. R. Kramer S. Weissmann, Prof., Dept. of Mechanics and Material Science, College of Engr. Piscataway, New Jersey 08854		8. CONTRACT OR GRANT NUMBER(s) N00600-77-C-1134
9. PERFORMING ORGANIZATION NAME AND ADDRESS David W. Taylor Naval Ship Research and Development Center Bethesda, Maryland 20084		10. PROGRAM ELEMENT, PROJECT, TASK AREA & WORK UNIT NUMBERS Project Element 61152N Task Area Z40220101 Work Unit 2802-004
11. CONTROLLING OFFICE NAME AND ADDRESS		12. REPORT DATE July 1982 13. NUMBER OF PAGES 19
14. MONITORING AGENCY NAME & ADDRESS(if different from Controlling Office)		15. SECURITY CLASS. (of this report) UNCLASSIFIED 15a. DECLASSIFICATION/DOWNGRADING SCHEDULE

16. DISTRIBUTION STATEMENT (of this Report)

APPROVED FOR PUBLIC RELEASE; DISTRIBUTION UNLIMITED

17. DISTRIBUTION STATEMENT (of the abstract entered in Block 20, if different from Report)

18. SUPPLEMENTARY NOTES

19. KEY WORDS (Continue on reverse side if necessary and identify by block number)

X-Ray Diffraction
Fatigue
Aluminum
Silicon

20. ABSTRACT (Continue on reverse side if necessary and identify by block number)

The distribution of dislocations in the surface layer and the interior of fatigued and stress-corrosion damaged specimen was determined by X-ray line broadening techniques. The data indicate that in both cases the dislocation density in the region of the surface is higher than that in the interior initially. With increasing damage the dislocation density in the interior increases rapidly and finally becomes equal to that of the

(Continued on Reverse Side)

DD FORM 1 JAN 73 1473 EDITION OF 1 NOV 65 IS OBSOLETE
S/N 0102-LF-014-6601

UNCLASSIFIED
SECURITY CLASSIFICATION OF THIS PAGE (When Data Entered)

(Block 20 continued)

surface. A crack or fracture occurs when this condition is fulfilled. The ratio of the dislocation density in the surface and the interior can provide a measure of the damage caused by fatigue and stress corrosion. Measurements of fatigue and stress-corrosion damage by the X-ray technique agreed closely with the measured damage.

TABLE OF CONTENTS

LIST OF FIGURES

LIST OF TABLES

NONDESTRUCTIVE METHOD FOR DETERMINING FATIGUE AND STRESS-CORROSION DAMAGE

I. R. Kramer

Technical Advisor
David W. Taylor Naval Ship R&D Center
Annapolis, Maryland 21402

and

S. Weissmann
Professor, Department of Mechanics and Material Science
College of Engineering
Piscataway, New Jersey 08854

Abstract

The distribution of dislocations in the surface layer and the interior of fatigued and stress-corrosion damaged specimen was determined by X-ray line broadening techniques. The data indicate that in both cases the dislocation density in the region of the surface is higher than that in the interior initially. With increasing damage the dislocation density in the interior increases rapidly and finally becomes equal to that of the surface. A crack or fracture occurs when this condition is fulfilled. The ratio of the dislocation density in the surface and the interior can provide a measure of the damage caused by fatigue and stress corrosion. Measurements of fatigue and stress-corrosion damage by the X-ray technique agreed closely with the measured damage.

Introduction

It is obviously very desirable to be able to determine by nondestructive methods the amount of fatigue and stress-corrosion damage. The ability to achieve these goals has not been attained to any considerable degree in spite of the considerable efforts devoted to the subject. In general, most of these investigations have been directed toward investigations concerned with microstructural or defect changes that occur in the bulk of the material, or such changes that occur at the surface, per se. One of the important points to be made in this paper is that fatigue and stress-corrosion damage may be determined when both the surface layer together with the bulk material are taken into consideration. Either taken separately may lead to erroneous conclusions.

In a series of investigations starting in 1961, it was shown that in the region of the surface to a depth in the range of 50 to 100 μm, the work-hardening was greater than that in the bulk of the material (1,2). This layer was also reported to form in fatigued specimens (3,4). It was further shown that in stress-corrosion cracking, those environments that caused damage also increased the work hardening of the surface region (5). These investigations led to the concept that the surface influences to a considerable degree, and in some cases controls, the dislocation generation in the bulk especially when the fatigue and stress-corrosion experiments are conducted below the macroscopic yield stress.

In a series of studies on aluminum 2024-T6, titanium (6Al/4V), and a 4130 steel the surface layer stress was measured as a function of the number of fatigue cycles under high-cycle conditions. The surface layer stress was defined as the additional stress required to produce a given amount of plastic deformation because of the extra work hardening in the surface layer. For these three classes of materials (fcc, hcp, bcc), a propagating crack formed whenever the surface layer stress attained a critical value for each material. This value was independent of the stress amplitude, the environment, and prior cyclic history. These observations are in agreement with the concept that crack formation at these low applied stresses is associated with an accumulation of dislocation of like sign (excess dislocations) in the surface layer (4,6). According to this concept, to form a crack, the surface layer acts as a barrier to a piled-up array or a local accumulation of dislocations of like sign and, at a sufficiently high applied stress and dislocation density, the stress field ahead of the "pile-up" exceeds the local fracture strength of the material. At low barrier strengths, plastic flow ahead of the "pile-up" occurs to allow stress relaxation. As will be discussed later in more detail, the formation of a surface layer containing a high density of dislocation is a necessary but not a sufficient condition for crack formation. It will be shown in those cases investigated that a crack forms when the dislocation density in the interior becomes essentially equal to that of the surface layer, and the dislocation density is essentially uniform throughout the cross section of the specimen.

X-Ray Diffraction Study of Surface Layer

X-ray diffraction analysis can provide a reliable method for the measurement of the changes in the dislocation density as a function of plastic deformation. The techniques are highly sensitive to the changes in the crystal structure and may be employed for a nondestructive evaluation. Both the double crystal diffractometer and the powder X-ray techniques have been employed in these investigations to determine the changes in the

dislocation density-depth profile of specimens subjected to tensile deformation and fatigue. The dislocation density, ρ, may be related to β, the widths of the X-ray line, or spots by (7):

$$\rho = \beta/bT, \tag{1}$$

where T is the subgrain size and b is the Burger's vector or

$$\rho = \beta^2/9b^2. \tag{2}$$

Equations (1) and (2) give the lower and upper bounds of the dislocation density, respectively. The dislocation density may be obtained from an analysis of the line profile (8) and the method of integral breadths (9). According to the latter

$$\beta \cos \theta = \frac{K\lambda}{L} + 4e \sin \theta, \tag{3}$$

where $e = \Delta d/d$ and d is the interplaner spacing. The first term on the right is related to the particle size while the second term is related to the microstrain $\langle \varepsilon^2 \rangle^{1/2}$. The dislocation density associated with the particle size and strain is, respectively

$$\rho_p = \frac{1}{L^2}, \tag{4}$$

$$\rho_\varepsilon = 12\langle \varepsilon^2 \rangle^{1/2}/b^2 \tag{5}$$

where $\langle \varepsilon^2 \rangle^{1/2} = e/1.25$ is the root mean square microstrain.

Dislocation-Depth Profile of Unidirectional Stressed Crystals

A somewhat typical X-ray line profile obtained for unidirectional strained metals is shown in Figure 1a for a silicon crystal that was strained 10% at 650°C. In this example, a double crystal diffractometer was employed. After the deformation, 100 μm was removed and it is apparent that the line sharpened considerably (Figure 1b). Figure 2 shows the dislocation density-depth profile (ρ-x) for silicon, a material with a low stacking fault energy; aluminum, a high stacking fault energy material; and gold, which exhibits little or no propensity for the formation of a surface oxide. To prevent possible relaxation effects in aluminum, the straining and X-ray measurements were carried out at -5°C. The ρ values given in Figure 2 and in the other portions of this paper were calculated from Equation (2). For all three metals, there was a decline by factors of 3 to 6 from the high surface layer density, ρ_s, to a constant value, ρ_i, at about 100 to 150 μm in the interior. These results, together with the published data, demonstrate that the work hardening even in unidirectional straining is not uniform throughout the cross section.

Dislocation Density-Depth Profile of Fatigued Specimens

Figure 3 shows data obtained by analysis of the surface layer, using shallow-penetrating copper radiation, ~7μm, after cycling specimens of aluminum 2024-T3 for various fractions of the fatigue life. The results are plotted for specimens with two average grain sizes differing by about 25% in grain diameter, and for tests carried out at two different stress

amplitudes. In agreement with Taira, et al (10, 11), the change in excess dislocation density during the life could be described by a three-stage sequence for all the tests. Rapid increases in the defect concentration occurred early (Stage I) and late (Stage III) in the life. A markedly decreased slope was obtained for the long duration of the second stage comprising the period from 0.15 to 0.95 N_f. All the data fell within the experimental error band, even for the alternate grain size stock, if a uniform shift factor related to the ratio of grain diameters was applied (12).

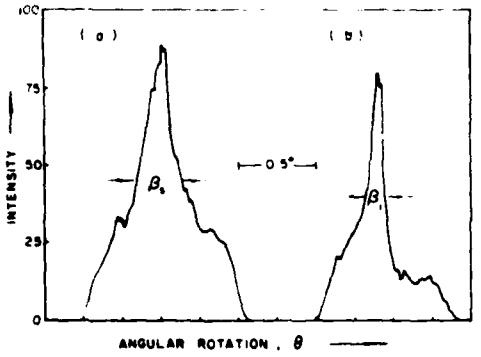

Figure 1 - X-ray rocking curve profiles of tensile deformed silicon single crystal. ϵ_p = 10% 650°C, tensile axis [110], (112) reflection, Cu Kα. (a) Original surface, (b) after removal of a 100 μm surface layer.

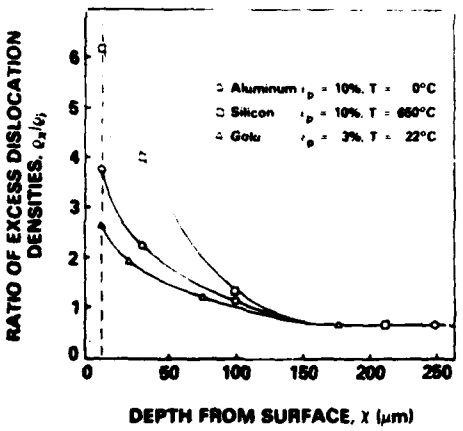

Figure 2 - Distribution of excess dislocations with depth from the crystal surface. Tensile axis and surface orientations: Al 100 and (100); Si 110 and (112); Au, 123 and (311)

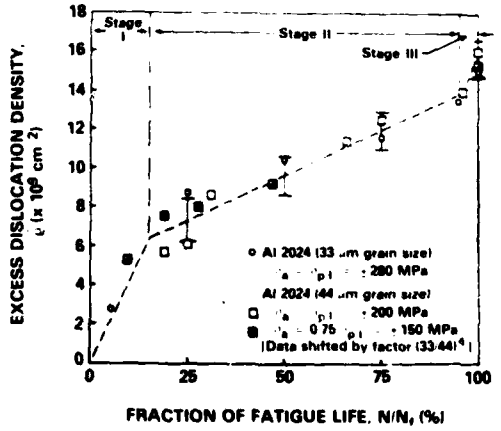

Figure 3 - Excess dislocation density in the surface for fatigued Al 2024-T3 specimens with G.S 4 and 33 mm, tested at various stress amplitudes. Cu Kα radiation.

The data presented in Figure 4a were obtained from the rocking curve analysis of aluminum 2024-T3 specimens cycled for various fatigue life fractions at ±200 MPa corresponding to the proportional limit. Analogous to the deformation characteristic of monotonically and cyclically deformed single crystals, the ρ-x profile revealed a higher excess dislocation density in the surface layer than in the bulk. Up to about 0.15% of the fatigue life (N = 21,000), the ρ-x profile was similar to that observed after single tension. Observations made after 5% of the fatigue life showed that the dislocation density in the bulk also increased, and a trough appeared on the ρ-x profile in the sub-surface region. With further cycling, the excess dislocation density continued to increase in the surface layer and in the bulk.

The data in Figure 5 were obtained for specimens of aluminum 2024-T4 fatigued in 3.5% NaCl in axial tension-tension. Except for the absence of a minimum, the curves are similar to those obtained for the axial tension-compression cases shown in Figure 4. At the lower damage level of 31% and 67% the β values to a depth of about 50 μm are greater than those in the bulk material. As the fatigue damage increased, the β values of the interior increased more rapidly than those of the surface, and again failure occurred when the two were essentially equal.

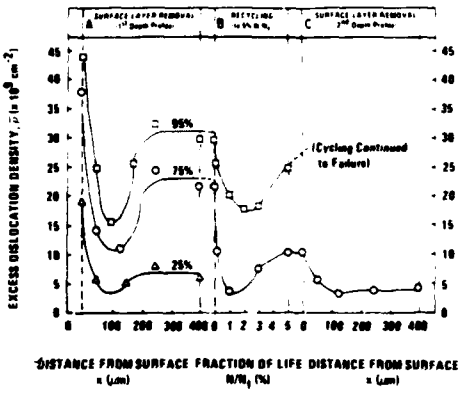

Figure 4 - (A) Excess dislocation density-depth profile for Al 2024-T3 specimens fatigued various percentages of life. (B) Dislocation density of surface after removal of surface layer and cycling. (C) Dislocation density - depth profile after fatiguing, N/N_f = 0.75, removal of surface and cycling N/N_f = 0.05.

Instability of Defect Structure in the Interior

From Figure 4 it is clear that ρ_s and ρ_i continue to increase with the amount of fatigue damage. The observation that ρ_i increases in the bulk appears to imply that permanent damage has occurred throughout the specimen, and yet it is known that the fatigue life of metals is completely recovered when the surface layer is removed periodically during the cycling process. The answer to this apparent conflict is that the defect structure in the interior is unstable without the presence of the surface layer. The instability of the interior defect structure is demonstrated in Figure 4b

by specimens that had been cycled 75% and 95% of their life and after removal of 400 μm were cycled again at the same stress (200 MPa). The dislocation density determined from the rocking curves employing copper radiation declined very rapidly during the initial recycling and, after about 200 cycles, reached a minimum that was approximately the same as that of the original specimen. After 1% to 2% of the life, ρ increased again. When the recycling was continued to 5% of the fatigue life, the ρ profile over the entire cross section was the same as that of the virgin specimen fatigued 5% of the life.

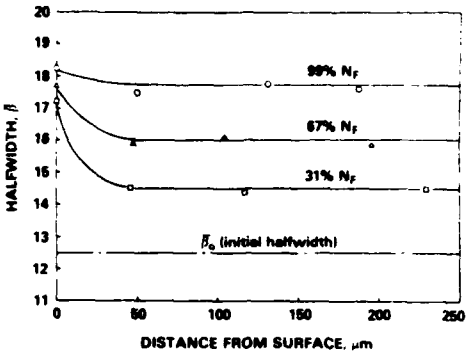

Figure 5 - β depth profile as a function of fatigue damage for Al 2024-T4 fatigued at 276 MPa in 3.5% NaCl. R = 0.1, Cr K_α

The reversion of the bulk dislocation content back to the virgin state when fatigued specimens were cycled in the absence of the work-hardened surface layer explains the extension of the fatigue life by periodic removal of the surface. The observations relative to this instability imply that there is a strong reaction of the dislocation in the interior to the surface layer. At the stress amplitude employed, it is apparent that the dislocation density in the bulk would not have increased during the cycling without the presence of the surface layer. In this sense, the increase in the bulk dislocation density is controlled entirely by the surface layer at least for high-cycle fatigue processes.

The instability observation has important implications relative to the influence of the environment on the work-hardening characteristics. The instability observations lead to the concept that the work-hardening of the interior is dependent on the surface layer. Accordingly, an environment that influences the surface layer will also affect the work-hardening of the bulk. For this to occur, the stress fields associated with the dislocation array in the surface layer must act over long distances. Conceivably, if the dislocations are arranged in a form similar to an inverse "pile-up," the stress may be transmitted over long distances. According to this model, the effective stress acting on the dislocations in the interior has, in addition to the applied stress, a stress component due to the dislocation array of the surface layer. The proposal that the stress field associated with the surface layer can act over a long distance to influence the plastic deformation of the bulk material finds support in the

investigations of Baranov, et al (13). Whereas it was previously shown that Stages I, II, and III were strongly influenced by removing the surface electrochemically during the deformation (14), these investigators reported that the surface removal also had a remarkable effect on the ductility of tungsten crystals. When no surface removal was involved, these single crystals normally failed in a brittle manner along (001) slip planes with a reduction in an area of about 12%. With surface removal, these crystals fractured with the formation of a neck and a reduction of an area of 83%. Apparently, since necking occurs when $d\sigma/d\varepsilon = \sigma$, the removal of the surface decreased the work-hardening of the entire specimen and local instability occurred at a stress much lower than the cleavage stress.

Dislocation Distribution in Surface and Bulk in Fatigue and Stress Corrosion

A very interesting and important aspect of fatigue failures as well as other subcritical crack formation such as stress-corrosion cracking and hydrogen embrittlement is that the cracks form at a relatively low stress level compared to the fracture stress of the material. It has been proposed (4,6) that such a crack can be formed by the pile-up of dislocation against or within the surface layer. According to this proposal, a crack would form when the surface layer became sufficiently strong to support a critical size pile-up. When the local stress associated with this accumulation of dislocations of like sign exceeds the fracture stress, a crack will form in the affected region. It should be noted that in Figure 3, and from Taira's results (10,11), fatigue failure occurred when the excess dislocation density attained a critical value, ρ^* or ρ^*, that was independent of the applied stress amplitude. It was also reported that propagating cracks formed when the surface layers reached a critical strength (6). The two cases are equivalent since $\sigma_s = G b \rho^{1/2}$. In this case, fracture occurred at the critical strength value independent of the environment, stress amplitude, and prior cyclic history. A necessary part of the surface layer fracture model is that a critical barrier strength is required to prevent relaxation of the stress fields. Fracture does not occur prior to the attainment of this critical strength, because the stress fields from the excess dislocations would be relaxed by plastic deformation. In fatigue processes where the direction of the dislocation motion changes with the direction of the applied stress, it is possible that stress relaxation can also occur.

It appears that in stress corrosion, the mechanism for damage may be similar to that occuring in fatigue. Figure 6 gives tha half width, β, as a function of distance from the surface for a 304 stainless steel stressed at 55% of the yield strength for various fractions of the cracking time, t/t_c, in 42% $MgCl_2$, where tc is the time to form a crack. The experimental data (15) show that a surface layer with a negative dislocation gradient is formed first. At $t_c = 0.1$, the β values in the interior are essentially the same as those of the unstressed material. With increasing exposure time in the $MgCl_2$ solution, the density of dislocation on the interior and the surface layer increases continuously. However, similar to the findings in fatigue, the increase in the β values in the interior is much more rapid than those at the surface. Again, similar to fatigue, cracking occurs when the values in the surface are essentially equal to those in the interior. In 1971, Kamachi and coworkers (16) showed (Figure 7) that the β values measured at the surface of 304 stainless steel specimen exposed to 42% $MgCl_2$ at various stresses increased continuously during the exposure time. The β values for specimens exposed to the same temperature and stress in an inert environment (parafin oil) increased relatively small amounts initially and after about 2 hours remained constant. It is apparent from

these results. that the environment caused a rapid increase in the generation of dislocations in the surface layer and in the interior as a consequence of the production of dislocations in the surface layer. Similar to the process proposed previously for fatigue (4) and stress-corrosion cracking (17,18), it appears that the stress field from dislocations in the region of the surface interacts with sources in the interior to cause a general increase in the dislocation density of the specimen as a whole.

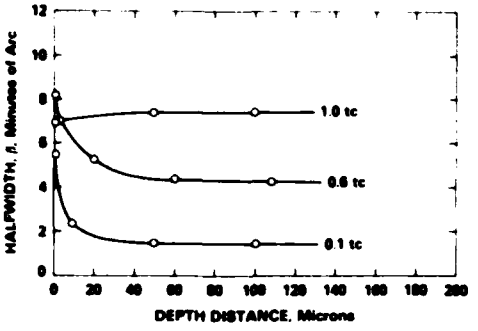

Figure 6 - β-x profile for 304 stainless steel stressed at 55% of the yield strength in $MgCl_2$ for various times

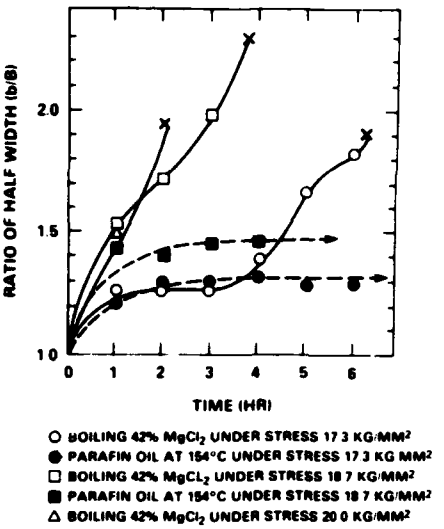

Figure 7 - β-time values measured at the surface for 304 stainless steel stressed in $MgCl_2$

Determination of Fatigue and Stress-Corrosion Damage

Of interest in Figure 3 is the observation that all the points fall on a single curve independent of the stress amplitude. Most importantly, a propagating crack apparently is initiated, and failure occurs when a critical value of the excess dislocation density, β^*, is attained. It is evident that if ρ^* can be determined, and the relationship between fatigue damage and the excess dislocation density is established, an assessment of the fatigue damage can be made. It may be seen from Figure 3, as well as from the data of Taira, et al (10,11), that the slope of Stage II is too low to be used for accurate and practical determination of fatigue damage. An examination of the depth profiles shown in Figure 4 reveals that the buildup of excess dislocation density at the surface layer occurs much earlier in the life than in the bulk. However, inspection of the plateau values, established at about 250 μm, discloses that the average excess dislocation density in the bulk increases steadily throughout the life. It follows that the fatigue damage can be determined, provided the X-ray beam penetrates sufficiently far into the materials to sample both the surface layer and bulk. Experimentally, for aluminum this can be achieved

by application of X-ray radiation with a short wavelength, such as molybdenum K_α radiation. Figure 8 exhibits a plot which compares the average excess dislocation densities obtained from measurements with copper and molybdenum radiation. It is seen that by applying molybdenum radiation, a sharp incline of the slope is obtained up to the critical value, ρ^*, and enables a determination of the accumulated damage unequivovally. By contrast, application of copper radiation, which samples only the defect structure of the quickly saturated surface layer, cannot accomplish this task, owing to the shallow slope during the intermediate life fractions. It is important to note that at $N/N_f = 1$, the ρ^*, values measured with molybdenum and copper radiation are equal. Since the former penetrates about 350 μm and the latter about 7 μm, the observation indicates that the dislocation density is uniform throughout the cross section of the specimen. It is also possible to estimate β^* from surface measurements. From Figure 3, when plotted in terms of β instead of ρ, the slope in the region from 25% to 95% damage is very low. Not too much error is made if the value for β is selected from these surface measurements, provided they are obtained in the region where the β values are increasing very slowly with the number of cycles. Of course, if a calibration curve such as in Figure 8 is available, then the damage may be read directly from the curve. In practice, it is unlikely that such a curve will be available. Yet another procedure may be used to determine whether to remove a part from service. Without actually knowing β^*, the part may be removed whenever the β_s/β_i value exceeds some prechosen value, for example, 0.9.

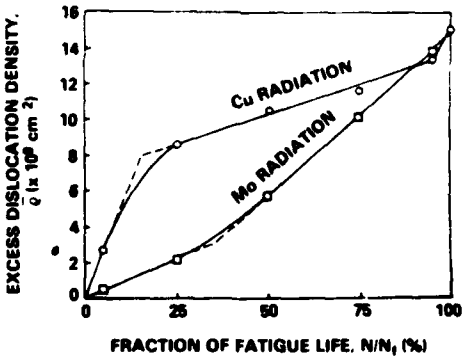

Figure 8 - Comparison of dislocation density measured with Cu and Mo radiation

To test the predictive capability of this method using the line-broadening method, specimens of aluminum 2024 were fatigued at four different stress amplitude blocks for varying number of cycles. X-ray line-broadening measurements were taken after each block using both copper and molybdenum radiation. From a calibration curve obtained from measurement taken at a single stress amplitude, as shown in Figure 8, the values

of N/N_f were obtained. The amount of fatigue after cycling at each block is shown in Columns 5 and 6 of Table I. At the end of the fourth cycling block, the specimens were fatigued to failure at a stress amplitude of 280 MPa to determine the remaining fatigue life. For specimens A and B, the X-ray line-broadening method predicted that the remaining fatigue life was 45% and 54%, respectively, compared to the measured values of 42% and 58%. The agreement is considered to be excellent. When Miner's method (19) is applied, the remaining life should have been 20%. A method for calculating fatigue damage based on the role of the surface layer proposed by Kramer (20) was used to calculate the damage reported in Column 4. The agreement between the actual and calculated fatigue damage is good.

Table I. Comparison of Cumulative Damage Estimates for Aluminum 2024 Spectrum Specimens Under High-Cycle Fatigue Condition

Cycling Block	Number of Cycles and Stress Amplitude	Expended Fraction of Life			
		Miner	Kramer	X-Ray DCD	
				Sample A	Sample B
1	36×10^3 cycles at ± 170 MPa+	0.20	0.20	0.19	0.15
2	7.5×10^3 cycles at ± 210 MPa+	0.40	0.31	0.29	0.30
3	3.0×10^3 cycles at ± 245 MPa+	0.60	0.49	0.41	0.38
4	1.5×10^3 cycles at ± 280 MPa+	0.80	0.63	0.55	0.46
5	Cycled to failure at ± 280 MPa	Remaining Life			
	Sample A: $N_5 = 3.19 \times 10^3$	X-ray DCD		0.45	0.54
	Sample B: $N_5 = 4.36 \times 10^3$	Actual (N_5/N_f)		0.42	0.58

In another series of tests, specimens of aluminum 2024-T4 were fatigued in a solution of 3.5% NaCl for various fractions of the life at three different stress amplitudes. In these experiments, chromium radiation was used and a calibration curve for β_{mo}/β_{cr} as a function of the fatigue damage, N/N_f was obtained. To test the predictive capability using an extrapolation technique the data were plotted in Figure 9, and a linear relationship was employed to determine the N/N_f values at β_{mo}/β_{cr} for equal to one. For the specimen fatigued at these three different stress amplitudes (241, 276 and 310 MPa), the intercept ranged between 94% and 98% and indicates that the linear extrapolation procedure is valid.

Recently, W. Mayo (21) investigated the fatigue behavior of aluminum 2024-T4 under low-cycle fatigue conditions in the tension-tension mode ($R = 0.2$). Unlike the case of high-cycle fatigue, the dislocation density in the interior was essentially equal to that of the surface for measurement obtained after cycling in excess of 25% of the fatigue life. The dislocation depth profile was not measured at lower percentages. Similarly, a 1020 steel fatigued under low-cycle conditions in axial tension-compression ($R = -1$) displayed a similar behavior at $N/N_f > 25\%$ (22). Nevertheless, as the fatigue damage was increased, the β values increased in a linear manner, and failure occurred at a critical value of β^* that appeared to be independent of the strain amplitude (0.6% to 1.0%). A linear relationship of β/β^* was used to calculate the remaining life of specimens that were fatigued under block-loading conditions of various strain amplitudes. These data are shown in Table II, where again the agreement between the actual and the predicted cycles remaining is good.

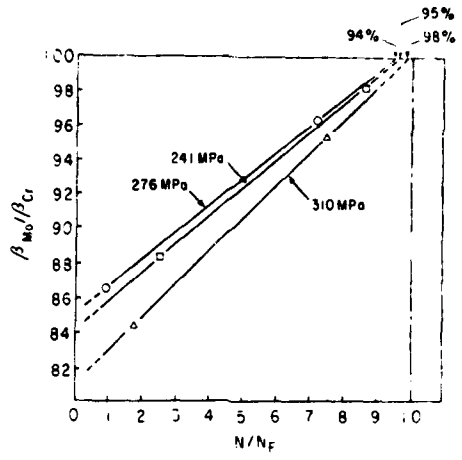

Figure 9 - Relationship between β_{Mo}/β_{Cr} and N/N_f for 2024-T4 Al in 3.5% NaCl

Table II. Comparison of Cumulative Damage for Aluminum 2024 Specimens Fatigued Under Low-Cycle Fatigue Conditions

Type of Loading	History	$\bar{\beta}$ Measured (minutes of arc)	Predicted Cycles Remaining	Actual Cycles
Monotonic	3,000 at 1.0% ε_{max}	22.09	4,550±1,550	6,430
Block	2,000 at 1.0% ε_{max} +10,000 at 0.6% ε_{max} +5,000 at 0.8% ε_{max}	19.65	26,025±5,225	27,285
Block	10,000 at 0.6% ε_{max} +2,000 at 1.0% ε_{max} +5,000 at 0.8% ε_{max}	22.09	22,230±3,230	19,842
Block	10,000 at 0.6% ε_{max} +5,000 at 0.8% ε_{max} +2,000 at 1.0% ε_{max}	18.89	26,600±3,230	22,730

The data for the prediction of stress-corrosion damage by X-ray technique is limited to 304 stainless steel exposed to 42% $MgCl_2$. An excellent correlation between the fraction of life time T/T_f and the ratio of the half width b/B was reported by Kamachi and coworkers (16), where b is the half width as a function of time, and B is the half-width of the original material measured at the surface (Figure 10). Note again, failure occurred at a constant value of b, independent of the applied stress. From Figure 6 it is also seen that the ratio of β_s/β_i would provide a measurement of the damage since failure would occur when $\beta_s = \beta_i$.

Acknowledgments

The authors gratefully acknowledge the support of this research by the David W. Taylor Naval Ship Research and Development Center.

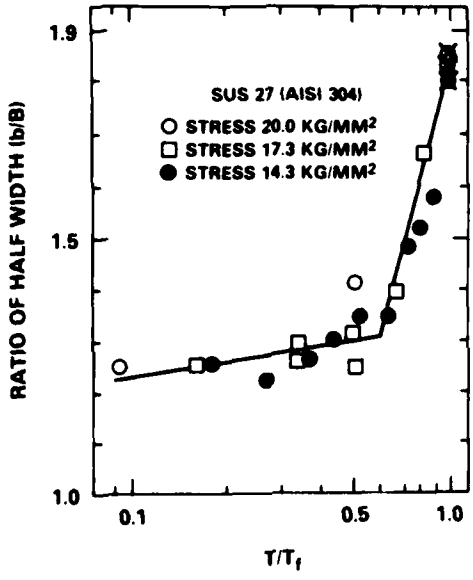

Figure 10 - Increase in the half-width as a function of the fraction of failure time T/T_f for 304 stainless steel subjected to stress corrosion in $MgCl_2$ at various stresses

References

1. I. R. Kramer and L. S. Demer, TMS-AIME, 221 (1961) p. 780.

2. I. R. Kramer, TMS-AIME, 230 (1964) p. 991.

3. H. Shen, S. F. Podleseck, and I. R. Kramer, Acta Met, 14 (1966) p. 341.

4. I. R. Kramer, Proc. Air Force Conf. on Fatigue, AFFDL-TR-O-144 (1969).

5. I. R. Kramer, Corrosion, 3 (11) (1975) p. 383.

6. I. R. Kramer, TMS-AIME, 5 (1974) p. 1735.

7. P. B. Hirsch, "Mosaic Structure," Progress in Metal Physics, 6 (1956) p. 236.

8. B. E. Warren and B. L. Averbach, Journal Applied Physics, 21 (1950) p. 595.

9. A. J. C. Wilson, X-Ray Optics, Methuen, London (1940) p. 37.

10. S. Taira and K. Hayaski, Proc. 9th Jap. Conf. on Testing Materials, 1 (1966).

11. S. Taira, K. Tanaka, and T. Tanable, Proc. 13th Jap. Congr. on Materials Research, 14 (1970).

12. S. Weissmann, R. Pangborn, and I. R. Kramer, Fatigue Mechanics, ASTM-STP-675, 163 (1979).

13. Yu. V. Baranov, E. P. Kostyukova and I. M. Makhmertov, Problemy Prochnosti (4) (Apr 1978) p. 483.

14. I. R. Kramer, TMS-AIME, 233 (8) (1965) p. 1462.

15. R. M. Yanici, S. Weissmann, and I. R. Kramer, Work in Progress (1979).

16. K. Kamachi, T. Otsu, and S. Obayaski, Journal Japan Inst. Metals, 35 (1971) p. 64.

17. I. R. Kramer and A. Kumar, Corrosion Fatigue, NACE-2 (1972) p. 146.

18. I. R. Kramer, Corrosion, 31 (1975) p. 383.

19. M. A. Miner, Journal Applied Mechanics, Series E-12 (1945) p. A-159.

20. I. R. Kramer, Proc. 2nd Int. Conf. on Mech. Behavior of Materials, 812 (1976).

21. W. Mayo, PhD Thesis, Rutgers University (1982).

22. I. R. Kramer, Work in Progress (1982).

INITIAL DISTRIBUTION

Copies

2 CNR
- 1 Code 465
- 1 Code 471

4 NRL
- 1 Code 6300
- 1 Code 6311
- 1 Code 6380
- 1 Code 6385

2 NAVAIR/AIR 320

1 NAVAL AIR DEVELOPMENT CENTER
NAVAL MATERIALS CENTER
WARMINSTER, PA 18974
ATTN: DR. F.W. WILLIAMS
CODE 606

5 NAVSEA
- 1 SEA 035
- 1 SEA 05D
- 1 SEA 323
- 2 SEA 99612

12 DTIC

1 AIR FORCE MATERIALS LABORATORY
WRIGHT-PATTERSON AF BASE
DAYTON, OH 45433
ATTN: DR. H. BURTE

1 NATIONAL BUREAU OF STANDARDS
WASHINGTON, D.C. 20234
ATTN: DR. JEROME KRUGER

1 CASE WESTERN RESERVE
MECHANICAL AND AEROSPACE ENGR.
CLEVELAND, OH 44106
ATTN: S.S. MANSON

1 UNIVERSITY OF CONNECTICUT
STORRS, CT 06268
ATTN: DR. A.J. EVILY

Copies

2 JOHNS HOPKINS UNIVERSITY
SCHOOL OF ENGINEERING
BALTIMORE, MD 21218
ATTN: DR. R. GREEN, R. POND

1 LEHIGH UNIVERSITY
327 SINCLAIR LAB., BLDG. 7
BETHLEHEM, PA 18015
ATTN: DR. R.P. WEI

1 UNIVERSITY OF MARYLAND
DEPT. OF CHEMICAL ENG.
COLLEGE PARK, MD 20740
ATTN: DR. R. ARSENAULT

3 MASSACHUSETTS INSTITUTE OF
TECHNOLOGY
CAMBRIDGE, MA 02139
ATTN: DR. R. LATANISON,
DR. N. SAKA
DR. M. COHEN

1 NORTHWESTERN UNIVERSITY
EVANSTON, IL 60201
ATTN: DR. J.B. COHEN

1 OHIO STATE UNIVERSITY
MET. ENGR. DEPT.
116 W. 19th AVENUE
COLUMBUS, OH 43210
ATTN: JOHN P. HIRTH

1 POLYTECHNIC INST. OF NEW YORK
333 JAY STREET
BROOKLYN, NY 11201
ATTN: DR. H. MARGOLIN

1 RENSSALAER POLYTECHNIC INST.
TROY, NY 12181
ATTN: DR. D.J. DUQUETTE

1 UNIVERSITY OF ROCHESTER
DEPT. OF MECHANICAL ENGR.
ROCHESTER, NY 14627
ATTN: DR. JAMES C. LI

Copies

10 RUTGERS UNIVERSITY
PISCATAWAY, NJ 08854
ATTN: DR. S. WEISSMANN

2 SYRACUSE UNIVERSITY
LINK HALL
SYRACUSE, NY 13210
ATTN: DR. Y. OSHIDA
DR. VOLKER WEISE

1 UNIVERSITY OF VIRGINIA
DEPT. OF APPLIED SCIENCES
CHARLOTTSVILLE, VA 22904
ATTN: DR. D.K. WILSDORF

1 CARNEGIE-MELLON UNIVERSITY
PITTSBURGH, PA 15213
ATTN: DR. J.C. WILLIAMS

2 UNIVERSITY OF ILLINOIS
DEPT. OF MET. AND MIN. ENG.
URBANA, IL 61801
ATTN: DR. H.K. BIRNBAUM
DR. C. ALTSTETTER

CENTER DISTRIBUTION

Copies	Code	Name
2	012	
2	17	
1	28	
1	280	
15	2802	
2	281	
6	282	
10	5211.1	Reports Distribution
1	522.1	Unclassified Library (C)
1	522.2	Unclassified Library (A)
2	5231	Office Services

DTNSRDC ISSUES THREE TYPES OF REPORTS

1. DTNSRDC REPORTS, A FORMAL SERIES, CONTAIN INFORMATION OF PERMANENT TECHNICAL VALUE. THEY CARRY A CONSECUTIVE NUMERICAL IDENTIFICATION REGARDLESS OF THEIR CLASSIFICATION OR THE ORIGINATING DEPARTMENT.

2. DEPARTMENTAL REPORTS, A SEMIFORMAL SERIES, CONTAIN INFORMATION OF A PRELIMINARY, TEMPORARY, OR PROPRIETARY NATURE OR OF LIMITED INTEREST OR SIGNIFICANCE. THEY CARRY A DEPARTMENTAL ALPHANUMERICAL IDENTIFICATION.

3. TECHNICAL MEMORANDA, AN INFORMAL SERIES, CONTAIN TECHNICAL DOCUMENTATION OF LIMITED USE AND INTEREST. THEY ARE PRIMARILY WORKING PAPERS INTENDED FOR INTERNAL USE. THEY CARRY AN IDENTIFYING NUMBER WHICH INDICATES THEIR TYPE AND THE NUMERICAL CODE OF THE ORIGINATING DEPARTMENT. ANY DISTRIBUTION OUTSIDE DTNSRDC MUST BE APPROVED BY THE HEAD OF THE ORIGINATING DEPARTMENT ON A CASE-BY-CASE BASIS.


DATE
ILME